Maham, Kinza; Kosonen, Vili; Peltoniemi, Juha; Kärhä, Petri; Ikonen, Erkki

Spectral analysis of deviations from key comparison reference values

Published in:
Metrologia

DOI:
10.1088/1681-7575/ad0c9e

Published: 02/02/2024

Document Version
Publisher's PDF, also known as Version of record

Metrologia

Spectral analysis of deviations from key comparison reference values

OPEN ACCESS
IOP Publishing | Bureau International des Poids et Mesures Metrologia
Metrologia **61** (2024) 015002 (7pp) https://doi.org/10.1088/1681-7575/ad0c9e

Spectral analysis of deviations from key comparison reference values

Kinza Maham[1,*], Vili Kosonen[1], Juha Peltoniemi[1], Petri Kärhä[1] and Erkki Ikonen[1,2]

[1] Metrology Research Institute, Aalto University, Espoo, Finland
[2] VTT MIKES, Espoo, Finland

E-mail: kinza.maham@aalto.fi

Received 11 June 2023, revised 25 October 2023
Accepted for publication 14 November 2023
Published 27 November 2023

Abstract

When studying the results of the key comparisons of spectral quantities, it appears that in many cases participants' results systematically deviate from the key comparison reference values over a limited spectral range. We carried out spectral analysis of such deviations in seven key comparisons of optical radiometry. The results reveal an approximate outcome that, on the average, each harmonic amplitude is inversely proportional to the order of the harmonic in all studied key comparisons. This new finding gives important information on the characteristics of spectral correlations. The result can be used in the uncertainty evaluation of spectral integrals, where the effect of unknown spectral correlations has earlier been challenging to assess quantitatively.

Keywords: correlated quantities, spectral irradiance, correlated color temperature, key comparison, uncertainty

1. Introduction

Optical radiometry measurements are crucial in many fields and industries, ranging from Earth observation to industrial applications. Therefore, the reliability of these measurements is of utmost importance. In order to assess the reliability of the optical radiometry measurements, Consultative Committee of Photometry and Radiometry (CCPR) key comparisons are conducted. These key comparisons allow a quantitative analysis of deviations from the key comparison reference value (KCRV) [1, 2]. The Key Comparison Database (KCDB), maintained by the Bureau International des Poids et Mesures (BIPM) [3], provides a large data set for spectral irradiance, spectral responsivity, and spectral diffuse reflectance comparison results. The results of these comparisons are widely considered to be the most reliable measurements in optical radiometry.

The KCRV, which is obtained through the key comparisons, serves as a valuable representation of the 'true' value in photometric and radiometric measurements. This is particularly important because the 'true' value is often unknown and difficult to determine. CCPR key comparisons provide a valuable data set for studying the characteristics of optical radiometry measurements.

This paper presents a working hypothesis that the spectral comparisons available in the KCDB offer reliable data for providing insights into the spectral correlations in optical radiometry measurements. The spectral analysis of deviations typically necessitates knowledge of the true value to determine the amplitudes of the deviations at different harmonic orders. We analyze the results of spectral comparisons and obtain new information on the spectral structure of deviations. We argue that this structure is present in any careful radiometric measurement of a spectral quantity. In

* Author to whom any correspondence should be addressed.

addition to improving understanding on spectral correlations of measured values, this finding can improve the reliability of the uncertainty analyses of spectrally integrated quantities. Earlier studies have highlighted challenges in estimating uncertainties of spectral integrals due to different correlation components [4–6].

2. Method

Figure 1 shows an example of deviations from the KCRV in the spectral irradiance comparison K1.a [7], fitted with three different functions. The fitting was done for the spectral range from $\lambda_1 = 250\,\text{nm}$ to $\lambda_2 = 2500\,\text{nm}$. The fitted curves shown in figures 1(a)–(c) are constructed by a sum of spectral components as

$$\delta(\lambda) = \sum_{i=0}^{N} A_i f_i(\lambda), \tag{1}$$

where A_i is the fitted amplitude of the ith harmonic component, the index set i includes 0, 1, 2, …, until the defined upper limit N, and the functions $f_i(\lambda)$ form an orthogonal basis when integrating over the wavelength from λ_1 to λ_2. The zeroth order basis function is always constant, $f_0(\lambda) = 1$.

Three different sets of orthogonal basis functions $f_i(\lambda)$ are used for fitting in figure 1. These basis functions are defined in terms of sinusoids, Chebyshev polynomials and Legendre polynomials as shown at low orders in figures 2(a)–(c), respectively. Sinusoidal basis functions with random phases ϕ_i have been used earlier in the analyses of the effects of unknown correlations [4]. Here we fit ϕ_i and use first sinusoids and Chebyshev polynomials

$$T_i(\lambda) = \cos\left[i \arccos\left(\frac{2\lambda - \lambda_1 - \lambda_2}{\lambda_2 - \lambda_1}\right)\right] \tag{2}$$

to define the basis functions [6]. Normalization of Chebyshev polynomials is provided by $g_i(\lambda) = T_i(\lambda)/\sigma_i$, where σ_i is the standard deviation of $T_i(\lambda)$ calculated over the spectral range from λ_1 to λ_2. Orthogonal basis functions then get the form

$$f_i(\lambda) = g_{(2i-1)}(\lambda)\cos\phi_i + g_{2i}(\lambda)\sin\phi_i, \quad i \geqslant 1. \tag{3}$$

Factors $\cos\phi_i$ and $\sin\phi_i$ define the weights of odd and even parts of the basis functions, respectively.

Figures 1(a) and (b) show the fitting results using sinusoidal and Chebyshev basis functions. Table 1 lists the fitted amplitudes and phases in the latter case with $N = 6$. Equation (3) with Chebyshev basis functions is an advantageous choice because the first order Chebyshev polynomial $T_1(\lambda)$ forms a constant slope as a function of wavelength. Equation (3) with Chebyshev polynomials then allows better fits to the deviations from the KCRV than the use of sinusoidal basis functions, which are periodical and must have the same value at λ_1 and λ_2. In practice, it is computationally efficient to use a recursive formula [8] to generate the Chebyshev polynomials instead of equation (2). The basis functions of equation (3)

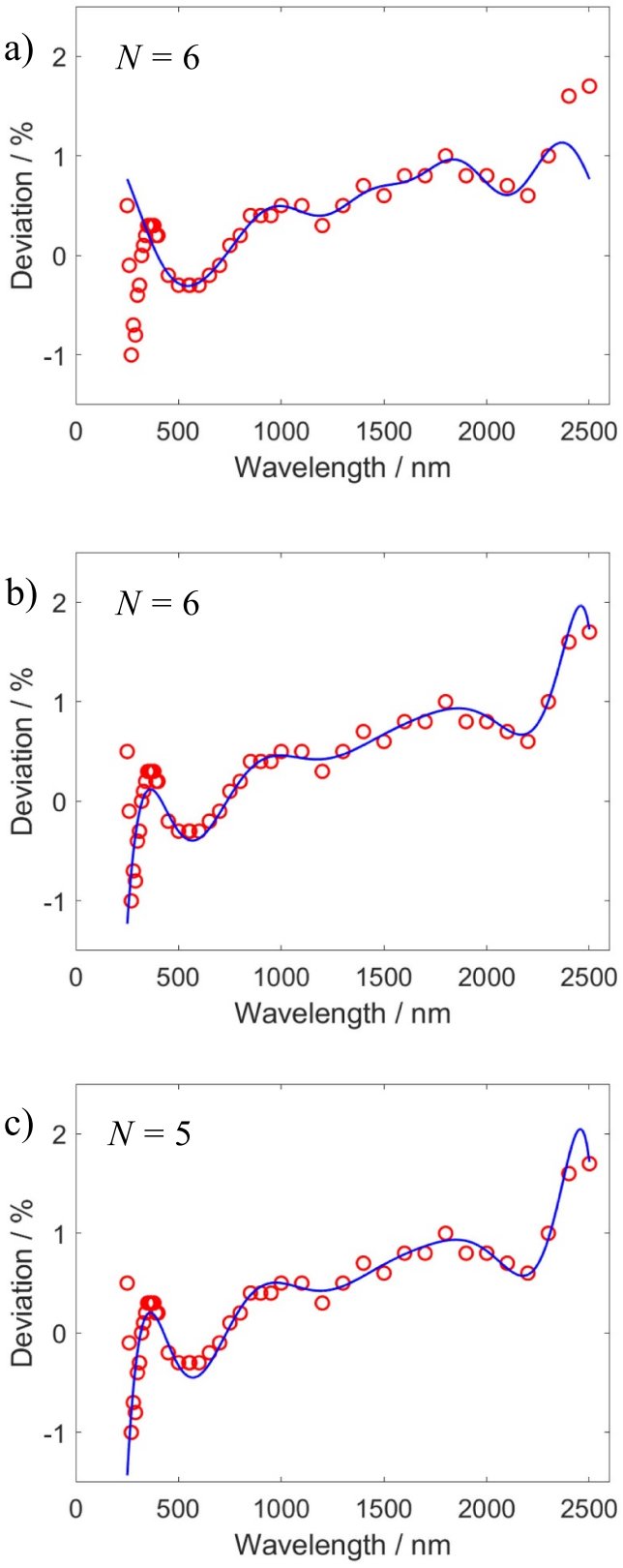

Figure 1. Deviations of a participant's data from KCRV in spectral irradiance comparison CCPR-K1.a (open circles). The solid lines are fits by equation (1) and functions based on (a) sinusoids, (b) Chebyshev polynomials, and (c) Legendre polynomials. The value of N is indicated in each case.

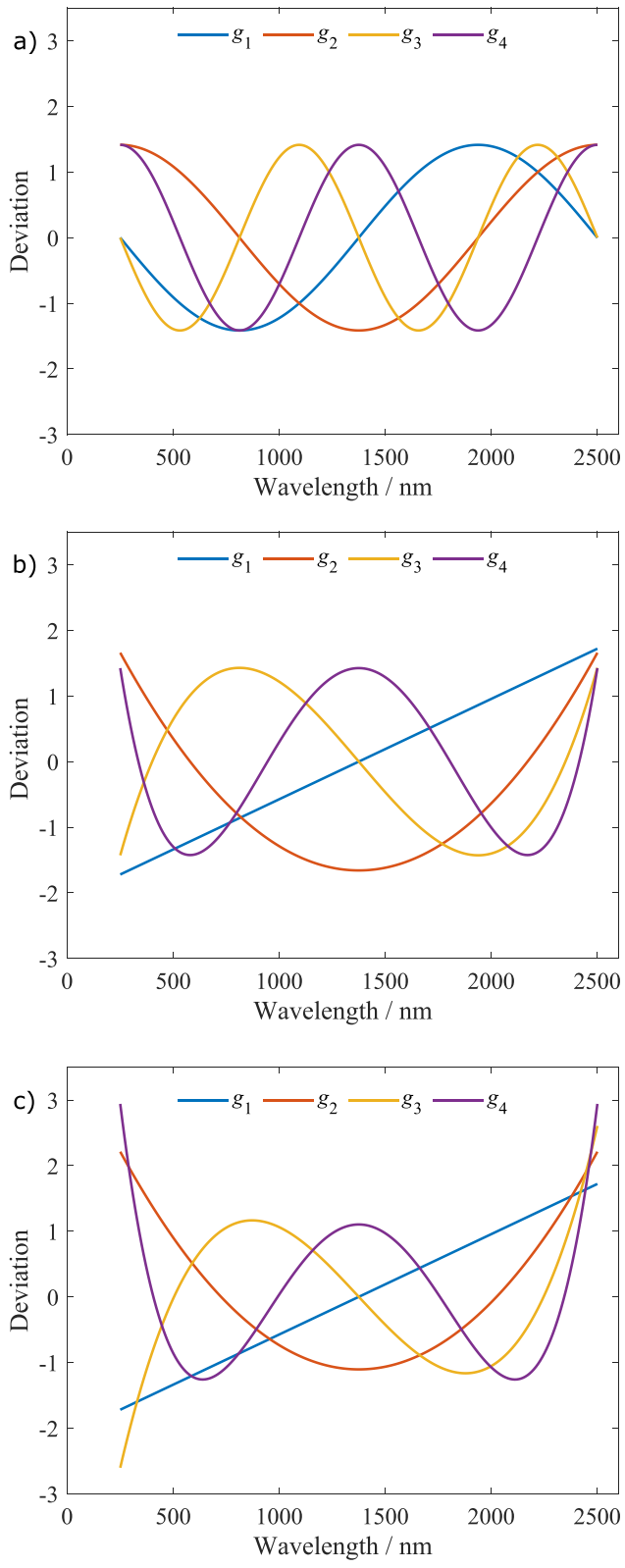

Figure 2. Comparison of functions $g_i(\lambda)$ of equation (3) in the case of (a) sinusoids, (b) Chebyshev polynomials, and (c) Legendre polynomials over the wavelength range 250 nm–2500 nm.

Table 1. Amplitudes and phases from the fit with basis functions defined in terms of Chebyshev polynomials in figure 1(b).

i	Amplitude A_i (%)	Phase ϕ_i (rad)
0	0.536	—
1	0.581	+0.016
2	0.183	+0.448
3	0.125	−0.512
4	0.200	−1.295
5	0.058	−1.158
6	0.024	+2.642

correspond to sinusoidal harmonics because each g_i function has the same number i of zero crossings.

Chebyshev polynomials are optimal for fitting purposes, as they minimize the oscillations in the fitted curve at high harmonic orders close to the borders of the spectral range [9]. We have also fitted the key comparison data using Legendre polynomials P_i instead of T_i, because orthogonality of Legendre polynomials is achieved with a weighting function which is equal to 1 over the whole spectral range of interest, in contrast to Chebyshev polynomials which require a non-constant weighting function. The constant weighting factor is important for the application of the results to uncertainty analysis of spectral integrals. Although the fits in figures 1(b) and (c) using Chebyshev and Legendre polynomials are both good, the value of N with Legendre polynomials must often be smaller than with Chebyshev polynomials to avoid exceedingly large oscillations close to the borders of the wavelength range.

The data points in figure 1 exhibit varying levels of uncertainty across different wavelength regions. To account for this, each data point was assigned a weight of $1/u_n^2$ in the fitting process, where u_n represents its uncertainty. Additionally, different data intervals were present in the ultraviolet (UV), visible, and infrared (IR) wavelength regions. To address this, the weight factors proportional to the data intervals were applied. For example, in figure 1 the data interval at UV wavelengths is 10 nm and at IR wavelengths 100 nm. Without weighting proportional to the data interval, the UV range would, in principle, have ten times more weight in the fitting than the IR range. The used relative weight for IR, corresponding to the usual weight $1/u_n^2$, is thus (100 nm) / (10 nm) = 10.

3. Results

Eleven participants of the spectral irradiance comparison K1.a had sufficient spectral coverage to use the methods of previous section in analysing the harmonic content of the deviations from KCRV. The Chebyshev fit results on mean amplitudes $\bar{A}_i$ of these eleven participants are shown in figure 3 on log-log scales. Fit of the line

$$\ln \bar{A}_i = a + b \cdot \ln i, \tag{4}$$

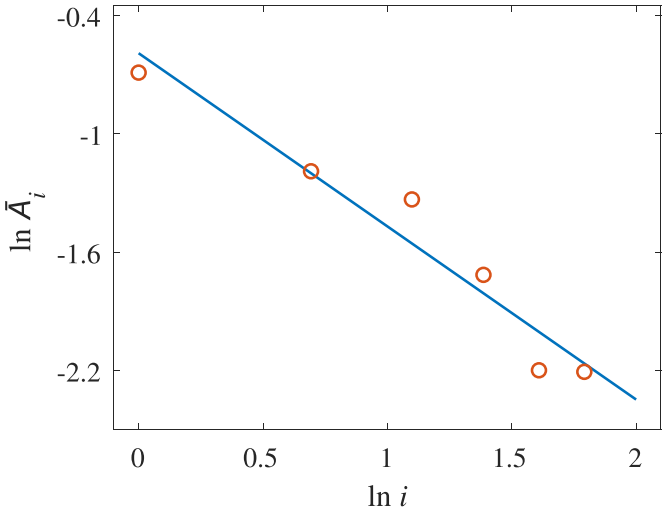

Figure 3. Logarithm of mean deviation amplitudes $\bar{A}_i$ of eleven participants at different Chebyshev basis function orders i in CCPR-K1.a key comparison [7]. The amplitude $\bar{A}_0$ is excluded from the data. The linear fit indicates a universal slope close to -1 observed in all studied key comparisons.

Table 2. Summary of the spectral analysis of deviations from the key comparison reference values. The number of the basis functions used is $N + 1$ and b is the slope describing the decay of the amplitudes of the basis functions (i.e. harmonics) with increasing order number.

Key comparison	Chebyshev polynomials N	Slope b	Legendre polynomials N	Slope b
CCPR-K1.a [7]	6	-0.88	5	-0.76
CCPR-K1.b [10]	5	-1.14	5	-1.03
CCPR-K2.a [11]	5	-0.90	4	-0.82
CCPR-K2.b [12]	5	-1.20	5	-0.86
CCPR-K2.c [13]	6	-0.95	4	-1.09
CCPR-K5(A) [14]	6	-1.01	5	-1.03
CCPR-K5(B) [14]	6	-1.17	5	-1.12
Average $\pm$ standard deviation		-1.04 ± 0.12		-0.96 ± 0.14

where a is the intercept, gives the slope $b = -0.88$ for the data of figure 3.

The KCDB contains data from five other CCPR key comparisons [10–14] which can be used for similar analysis as carried out for K1.a. The results are shown in table 2 for the slope parameter b using both Chebyshev and Legendre basis functions. For some comparisons, the number of spectral points was low, and the number of the basis functions could be extended only up to $N = 5$ or $N = 4$ in the case of Chebyshev or Legendre polynomials in equation (1). The report on the spectral diffuse reflectance comparison K5 [14] contains two different data sets A and B, which are here treated as separate comparisons.

Different weighting methods in the fitting process may in principle introduce hidden biases in the results. We made various test to study the presence of such effects. For example, we carried out fitting without weighting proportional to the data interval as described in section 2. The difference between the values of the slope b obtained with and without the weight related to the data interval was less than 0.01.

Various tests of synthesizing key comparison results by random numbers were also made. A synthetic comparison is an imaginary comparison where the results are artificially generated by a computer using the defined probability distribution function. Figure 4 shows the mean harmonic amplitudes of 10 synthetic key comparisons of 10 participants with measurements at 20 wavelengths. The result of each participant at each wavelength was randomly selected from a zero-mean Gaussian distribution with unity variance, after which equations (1) and (3) with Chebyshev polynomials were fitted to the results to determine harmonic amplitudes A_i of each participant. The harmonic amplitudes were averaged over all participants and comparisons to obtain $\bar{A}_i$. The fit by equation (4) then gave slope $b = 0.04$. Similar small values of the slope parameter were obtained in additional tests with synthetic key comparisons, where the uncertainties were different in different wavelength ranges.

4. Discussion

The slope parameters of all key comparisons of table 2 are roughly equal. For Chebyshev (Legendre) polynomials, the average slope is $b = -1.04$ (-0.96) with the standard deviation of 0.12 (0.14) in the sample of seven comparisons. The analysis with Legendre polynomials uses lower values of N and results with less negative average slope with higher standard deviation, but the differences are not statistically

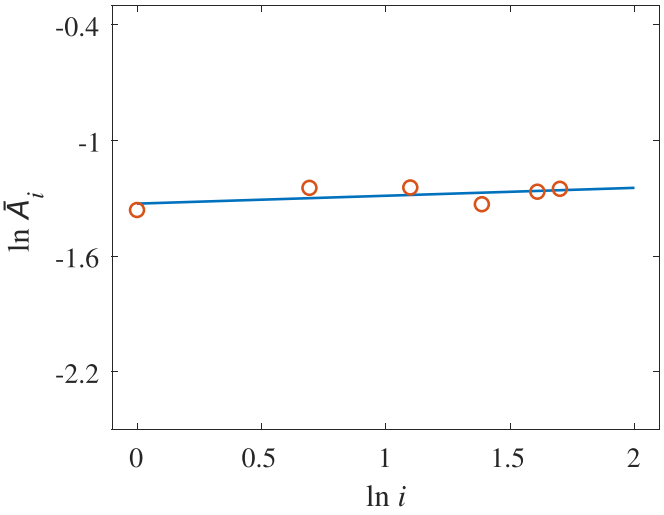

Figure 4. Mean deviation amplitudes from synthetic comparisons where the result of each participant is taken from a zero-mean Gaussian distribution with unity variance.

significant with this low number of available key comparisons. When sinusoidal basis functions are used, the average slope parameter becomes $b = -0.77$, corresponding to the inability of sinusoidal functions to fit properly sloped data at the borders of the wavelength range. According to equation (4) the average amplitude of the basis functions is proportional to i^b or approximately $\bar{A}_i \simeq \bar{A}_1/i$, when $b \cong -1$, as indicated by the average slopes in table 2. The observed power law corresponds to $1/f$ noise because the harmonic order i is proportional to the oscillation frequency of the basis functions. In the case of figure 4, $b \simeq 0$ and there is no dependence of the amplitude on harmonic order i, i.e. the amplitudes are random, as they should be in the case of synthetic comparisons.

The observed spectral structure in the deviations from KCRV appears to be new and universal. It applies at least to all available CCPR key comparisons. It can be concluded that such spectral structure probably exists in the average results of all careful spectral measurements in radiometry.

Although the deviations from the true value are smaller than the measurement uncertainty, the revealed spectral structure may lead to (unknown) correlations between the values measured at close-by wavelengths. This finding has implications to the uncertainty evaluation of spectral integrals, where the largest contribution comes from partial correlations [4, 6]. The universal power law $\bar{A}_i \propto 1/i$ allows to improve the reliability of the determined uncertainties, because the earlier rough assumption of equal probability of fully correlated, partially correlated and non-correlated uncertainty contributions can be replaced by a more quantitative approach. Appendix gives a practical example how the uncertainty analysis of a ratio of spectral integrals can be carried out using the new information.

5. Conclusion

After reviewing the outcomes of various spectral comparisons, we observed in many cases a consistent deviation from the reference value in a particular spectral range. To investigate these deviations further, we conducted a spectral analysis, which disclosed that the average amplitude of each harmonic is inversely proportional to its order in all key comparisons studied. Various tests with synthetic random data did not reproduce such features and thus confirm that the harmonic structure is an intrinsic property of spectral radiometric data. A possible reason for this harmonic structure is that the spectral comparisons extend to the limits of the spectral range where measurements start to become difficult. For example, when measuring the silicon photodiode spectral responsivity, accurate measurements become more difficult when approaching shorter wavelengths in the UV range and longer wavelengths in the IR range. Probable deviations close to the limiting wavelengths cause deviations which may be described by slopes and parabolic shapes whereas spectral deviation shapes with many zero crossings are not expected to occur frequently.

This new finding is significant in comprehending the nature of spectral correlations and can aid in the assessment of uncertainties of spectral integrals, which was previously challenging to do quantitatively due to the unknown spectral correlations. Furthermore, our application of a newly formulated deviation function for computing uncertainties in correlated color temperature has solved previous problems in weighting different uncertainty contributions in spectral integrals. Finally, our findings are not necessarily limited to radiometric measurements as a function of wavelength, but similar features may appear in measurements of other quantities as a function angle, time or other continuous variable.

Acknowledgment

The Project 19ENV04 Metrology for Aerosol Optical Properties (MAPP) leading to this publication has received funding from the EMPIR programme co-financed by the Participating States and the European Union's Horizon 2020 research and innovation programme. This work is partly funded by the Academy of Finland Flagship Programme, Photonics Research and Innovation (PREIN), decision Number: 320167. We thank Sami Talvitie for developing the fitting software especially in the case of Legendre polynomials.

Appendix A

A.1. Application to uncertainty analysis of correlated color temperature

Kärhä *et al* [4] previously computed the uncertainties related to the correlated color temperature (CCT) for a light source that corresponds to the CIE Standard Illuminant A [15]. CCT is a quantity which essentially depends on ratios of spectral integrals. Detailed calculation of the CCT is available in several sources, including Durmus [16], McCamy [17], and Hernandez-Andres *et al* [18]. In this appendix

we study how the results of [4] change when the harmonic amplitudes of the deviation function are assumed to be inversely proportional to the harmonic order. As in [4], we assume a constant relative standard uncertainty $u_c(\lambda)$ of 1% of spectral irradiance values across the entire wavelength range from $\lambda_1 = 360\,\text{nm}$ to $\lambda_2 = 830\,\text{nm}$ at 1 nm intervals.

In the Monte Carlo analysis, possible spectral correlations are considered by combining spectral basis functions in a specific way to create varying wavelength dependent deviation functions, consistent with the uncertainty estimates of the input quantities. Specifically, the MC method generates a large number of random samples of the input variables, each of which is distorted based on the spectral deviation functions to create a perturbed input dataset. The perturbed dataset is then used to compute the corresponding output variables, resulting in a distribution of output values that reflects the uncertainty and variability of the input quantities [19]. This distribution can be analyzed statistically to obtain the estimates of the mean, variance, and other higher-order moments of the output variables, as well as their probability density functions and confidence intervals.

The deviation function $\delta(\lambda)$ distorts the spectrally varying input quantities as

$$E_e(\lambda) = [1 + \delta(\lambda) \cdot u_c(\lambda)] \cdot E(\lambda), \tag{A.1}$$

where $E(\lambda)$ is the nominal spectral irradiance and $E_e(\lambda)$ is the distorted spectral irradiance. According to the results in table 2, the deviation function is assumed to follow equation (1) with $A_i \propto 1/i$ for $i \geqslant 1$. Legendre polynomials with $g_i(\lambda) = P_i(\lambda)/\sigma_i$ are used to construct the basis functions $f_i(\lambda)$. Then the normalization condition $\sum_{i=0}^{N} A_i^2 = 1$ can be used to obtain the deviation function

$$\delta(\lambda) = A_0 + A_1 \cdot \sum_{i=1}^{N} \frac{1}{i} \cdot f_i(\lambda), \tag{A.2}$$

where $A_0 = \sin\phi$,

$$A_1 = \frac{\cos\phi}{\sqrt{\sum_{i=1}^{N} \frac{1}{i^2}}} \tag{A.3}$$

and ϕ is random phase from a uniform distribution between $-\pi$ and π. The range of parameter N spans from 1 up to the value of the Nyquist criterion $N = 235$ [4]. At large values of N, the sum of inverse-squared integers approaches $\pi^2/6$. The orthogonal basis functions $f_i(\lambda)$ used for the MC analysis are given by equation (3), where the phases ϕ_i get random values from a uniform distribution between $-\pi$ and π.

The quantitative relation between slope $b = -1$ and spectral correlation in irradiance values is given by equations (A.1)–(A.3). The shape of the deviation function $\delta(\lambda)$ is such that neighboring spectral irradiance values are probably deviated to the same direction from the reference value. This behavior is most pronounced at low harmonic orders $i = 1$, 2 and 3, which have the highest weights $1/i$. However, the detailed shape of the deviation function remains unknown, but is covered by the Monte Carlo simulation.

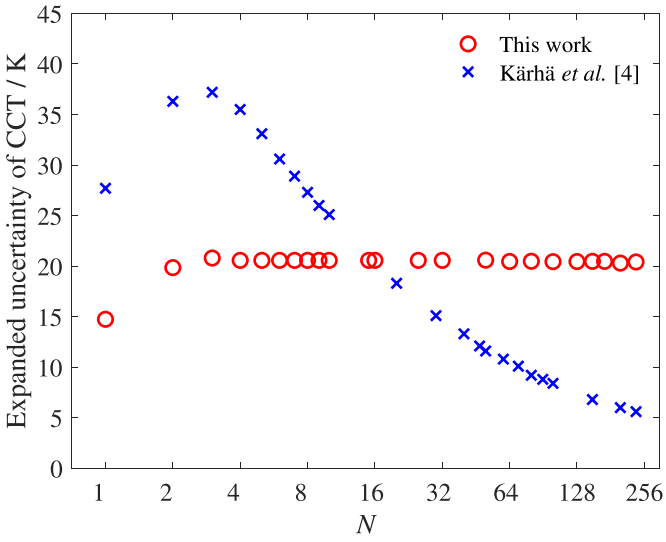

Figure A.1. Expanded uncertainty of CCT as a function of N. The uncertainties reported in [4] are depicted as crosses, while our uncertainties are shown as circles.

Figure A.1 shows the comparison between the expanded uncertainties derived by Kärhä *et al* in [4] and those obtained with the new deviation function of equation (A.2). Figure A.1 displays the cumulative uncertainty as each harmonic component up to N is included in the calculation. The deviation amplitudes in [4] have no other limitation than that the sum of squares of the amplitudes is normalized to 1. Thus the uncertainty reduces with increasing N, because of emerging higher harmonics which change CCT only little. It was assumed that the probable uncertainty of CCT is the average of the uncertainties obtained at $N = 0$, at $N = 235$, and at the value of N where the effect of the deviation function is most severe. The above values of N correspond to full correlation of spectral data, fully uncorrelated spectral data, and the worst case of partial spectral correlation, respectively. The assumption of equal weights of different correlation cases leads to the CCT expanded uncertainty of 14 K [4].

As compared with the method of [4], the lower harmonic orders are dominating in equation (A.2). Figure A.1 shows that the uncertainty converges to a specific value with large values of N, resulting in an expanded uncertainty of 20 K for CCT. The approach of equation (A.2) provides a more robust measure of the true uncertainty associated with CCT, determined from spectral irradiance measurements, than the method of [4]. The uncertainty estimates of this work and of [4] deviate by 6 K, but the new value of 20 K is more reliable, because it is based on improved knowledge on partial spectral correlations which affect the quantities defined in terms of ratios of spectral integrals. If it is assumed that $A_0 = A_1$, MC simulation gives an expanded uncertainty of 21 K for the CCT, showing

that the uncertainty is not sensitive to the value of the zeroth order amplitude.

ORCID iDs

Kinza Maham https://orcid.org/0000-0001-6740-1317
Juha Peltoniemi https://orcid.org/0000-0001-8444-0879
Petri Kärhä https://orcid.org/0000-0002-4774-7887
Erkki Ikonen https://orcid.org/0000-0001-6444-5330

References

[1] CIPM MRA 1999 Mutual recognition of national measurement standards and of calibration and measurement certificates issued by national metrology institutes (International Committee of Weights and Measures (CIPM)) (available at: www.bipm.org/en/cipm-mra/cipm-mra-documents)
[2] CIPM 2021 Measurement comparisons in the CIPM MRA, Guidelines for organizing, participating and reporting (CIPM MRA-G-11) (available at: www.bipm.org/documents/20126/43742162/CIPM-MRA-G-11.pdf/)
[3] (Available at: www.bipm.org/kcdb/comparison/quick-search)
[4] Kärhä P, Vaskuri A, Mäntynen H, Mikkonen N and Ikonen E 2017 Method for estimating effects of unknown correlations in spectral irradiance data on uncertainties of spectrally integrated colorimetric quantities *Metrologia* **54** 524–34
[5] Kärhä P, Vaskuri A, Pulli T and Ikonen E 2018 Key comparison CCPR-K1.a as an interlaboratory comparison of correlated color temperature *J. Phys.: Conf. Ser.* **972** 012012
[6] Vaskuri A, Kärhä P, Egli L, Gröbner J and Ikonen E 2018 Uncertainty analysis of total ozone derived from direct solar irradiance spectra in the presence of unknown spectral deviations *Atmos. Meas. Tech.* **11** 3595–610
[7] Woolliams E R, Fox N P, Cox M G, Harris P M and Harrison N J 2006 Final report on CCPR-K1.a: spectral irradiance from 250 nm to 2500 nm *Metrologia* **43** 02003
[8] Smith I M and Forbes A B 2018 Algorithms and software for fitting polynomial functions constrained to pass through the origin *J. Phys.: Conf. Ser.* **1065** 212022
[9] Bayliss A and Turkel E 1992 Mappings and accuracy for Chebyshev pseudo-spectral approximations *J. Comput. Phys.* **101** 349–59
[10] Sperfeld P 2008 Final report on the CIPM key comparison CCPR-K1.b: spectral irradiance 200 nm to 350 nm *Metrologia* **45** 02002
[11] Brown S W, Larason T C and Ohno Y 2010 Final report on the key comparison CCPR-K2.a-2003: Spectral responsivity in the range of 900 nm to 1600 nm *Metrologia* **47** 02002
[12] Goebel R and Stock M 2004 Report on the comparison CCPR-K2.b of spectral responsivity measurements in the range 300 nm to 1000 nm *Metrologia* **41** 02004
[13] Werner L 2014 Final report on the key comparison CCPR-K2.c-2003: spectral responsivity in the range of 200 nm to 400 nm *Metrologia* **51** 02002
[14] Nadal M, Eckerle K L, Early E A and Ohno Y 2013 Final report on the key comparison CCPR-K5: spectral diffuse reflectance *Metrologia* **50** 02003
[15] CIE 15 2004 *Technical Report-Colorimetry* 3rd edn (Comission Internationale de l'Eclairage) p 72
[16] Durmus D 2021 Correlated color temperature: use and limitations *Light. Res. Technol.* **54** 363–5
[17] McCamy C S 1992 Correlated color temperature as an explicit function of chromaticity coordinates *Color Res. Appl.* **17** 142–4
[18] Hernández-Andrés J, Lee R L and Romero J 1999 Calculating correlated color temperatures across the entire gamut of daylight and skylight chromaticities *Appl. Opt.* **38** 5703–9
[19] JCGM 101 2008 *Evaluation of Measurement Data–Supplement 1 to the 'Guide to the Expression of Uncertainty in Measurement'. Propagation of Distributions Using a Monte Carlo Method* (Joint Committee for Guides in Metrology (JCGM)) p 82